

Change of Venous Susceptibility upon Visual Activation: 3D Multi-echo GRE vs. GRE-EPI Functional QSM

PINAR SENAY ÖZBAY^{1,2}, Cristina Rossi¹, Geoffrey Warnock³, Felix Kuhn³, Klaas Paul Prüssmann², and Daniel Nanz¹

¹Department of Radiology, University Hospital Zürich, Zürich, Switzerland, ²Institute of Biomedical Engineering, ETH Zürich, Zürich, Switzerland, ³Department of Nuclear Medicine, University Hospital Zürich, Zürich, Switzerland

Target Audience Researchers who are interested in fMRI, Quantitative Susceptibility Mapping and processing of phase data.

Background In functional MRI, the magnitude of T2*-weighted images is used to map areas of brain activation. Besides the magnitude, also the phase of the complex MR signal has been shown to vary with neuronal activity levels¹. Phase data also allow a quantification of magnetic susceptibility differences by Quantitative Susceptibility Mapping (QSM), which was shown to provide measures of susceptibility changes coupled to neuronal activation²⁻⁵. So far, functional QSM (fQSM) relied on data acquired with fast Echo Planar Imaging (EPI) readout²⁻⁵ which can generate fQSM time series with a good temporal resolution. However, the poor EPI image quality and the fast signal decay that occurs in areas of strong field inhomogeneity may compromise the susceptibility quantification⁶.

Purpose A recent review⁷ discussed the use of 3D GRE sequences in susceptibility-based functional studies. In this study we investigate the potential advantage of a 3D multi-echo gradient recalled echo (GRE) data acquisition over an EPI acquisition for the evaluation of neuronal activation patterns and quantitative susceptibility changes induced by visual stimulation assessed with techniques of QSM.

Materials and Methods Experimental Design: Three healthy volunteers participated in this IRB approved study. For each volunteer, visual stimulation was performed at 3 Tesla in two experimental setups. **Experiment 1 (Exp1)** consisted in the acquisition of 3D multi-echo GRE data (GRE) (7TE, $\Delta TE=10$ ms, $TE_1 = 5.3$ ms, TR = 75 ms, FA = 50°, voxel size: 0.58 x 0.58 x 1.2 mm) during prolonged (4:56 minutes) visual stimulation and at rest, respectively. In **Experiment 2 (Exp2)**, 80 single-echo gradient-echo EPI (EPI) scans (TE = 35ms, TR = 3 s, voxel size: 1.8 x 1.8 x 4 mm) were acquired during 8 epochs, in which 5 scans of visual stimulation were alternated with 5 scans of rest condition, with a total experiment time of 4 minutes. T1-weighted images (3D Turbo-Field-Echo sequence, TE = 4.22ms, TR = 9.09 ms, FA = 8°, voxel size: 0.43 x 0.43 x 0.9 mm) were acquired for anatomical reference. **Visual Paradigm:** The visual stimulation involved presenting a black and white polar checkerboard on grey background reversing at a frequency of 8 Hz, while at rest a grey screen with a red focus crosshair was presented. **Data Processing: QSM** For Exp1, maps of wrapped phase increments per ΔTE were calculated from the multi-echo complex data according to $WPI_w = \text{angle}(\frac{1}{N-1} \sum_{n=1}^{N-1} S_n^* S_{n+1})$ [Eq. 1]. The phase was unwrapped and background-fields were removed with the Laplacian-based SHARP (threshold parameter = 0.1) method using the relation: $L(WPI) = \cos(WPI_w) \cdot L(\sin(WPI_w)) - \sin(WPI_w) \cdot L(\cos(WPI_w))$ (Eq. 1). Background noise and convolution artifacts were reduced by element-wise multiplication with a binary whole-brain mask eroded by 3 voxels. Quantitative susceptibility, ΔX , maps were obtained from the unwrapped, high-pass filtered phase images (SHARP⁸) by dipolar inversion, using the relation $\Delta X = FT^{-1}(\frac{FT(-SHARP(\gamma B_0 \Delta TE))}{g})$, $g = \frac{1}{3} - \frac{k_z^2}{k^2}$, $k^2 = k_x^2 + k_y^2 + k_z^2$, where FT = Fourier Transform, γ = gyromagnetic ratio, B_0 = field strength, ΔTE = echo-time increment. Division by zero-values in dipole-kernel, g , was avoided by thresholding and regularization^{8,9}. For Exp2, susceptibility maps were computed in an equivalent way but with the single-echo phase images as input to Eq. 1.

Statistical Parametric Maps, Exp2 SPM8¹⁰ was used for single-subject analyses for both, the magnitude and the QSM time-series images⁵. Pre-processing of magnitude and QSM data included realignment and co-registration to the anatomical reference, segmentation, normalization, Gaussian smoothing, and temporal high-pass filtering. A T1-weighted image (Anatomy) was co-registered and re-sliced to match the T-score map data. T-score maps of BOLD and QSM data were overlaid on Anatomy (Fig. 1).

Difference maps For both experiments, susceptibility-difference maps were calculated as $\Delta \Delta X = \Delta X_{on} - \Delta X_{off}$. For Experiment 2, average ΔX_{on} and ΔX_{off} maps were computed by averaging all time-series images acquired during visual stimulation or at rest, respectively.

RoI analysis For each volunteer, susceptibility differences induced by the visual stimulation in the sagittal sinus and in lateral veins were computed for both experiments. Four regions of interest were placed over the sagittal sinus and over other large cerebral veins (red circle in Fig. 2d). Mean values and standard deviations in ppb (SI units) are given in Table 1. Statistical significance test has been also done between susceptibility differences (t-test unpaired one-tailed, $p < 0.01$).

Results SPM-derived activation maps for magnitude and QSM data of Exp2 highlighted areas of the visual cortex (Fig. 1). fQSM activation patterns (hot) showed highly localized changes, compared to BOLD (yellow), mostly surrounding the veins supplying the visual cortex (Fig. 1). The susceptibility changes were in agreement with published value ranges for both experiments³ and the RoI analysis (Table 1) showed significantly higher susceptibility differences in data computed from Exp1 as compared to Exp2. Exp1 provided superior image quality of the susceptibility maps which resulted in a better visibility of the vasculature in the GRE data set as compared to the EPI data set in Exp2 (Fig. 2 a, b). Difference maps allowed the identification of veins with a stimulation-induced reduction of magnetic susceptibility in both experiments (Fig. 2c, d). The changes in susceptibilities within regions of interests (sagittal sinus (V1), and cerebral vein (red circle, Fig. 2(d) - V2)) are shown in Table. 1, for all volunteers and acquisitions (EPI vs. GRE).

Table. 1 Reduction of venous susceptibility induced by visual stimulation as measured by EPI- and GRE-based QSM within the sagittal sinus (V1) and the cerebral vein (V2) shown in Fig. 2d. in ppb.

| Volunteer | $\Delta \Delta X_{EPI}$ | | $\Delta \Delta X_{GRE}$ | |
|-----------|-------------------------|---------|-------------------------|---------|
| | V1 | V2 | V1 | V2 |
| 1 | -22 ± 3 | -19 ± 1 | -33 ± 8 | -31 ± 5 |
| 2 | -20 ± 3 | -6 ± 1 | -32 ± 1 | -26 ± 4 |
| 3 | -22 ± 5 | -20 ± 2 | -29 ± 7 | -28 ± 5 |

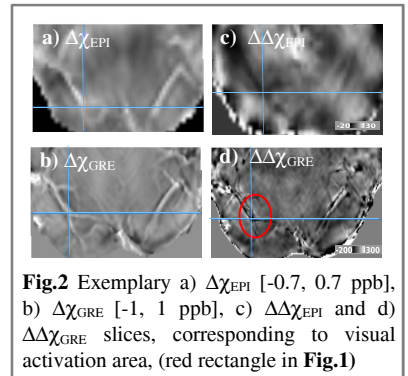


Fig.2 Exemplary a) ΔX_{EPI} [-0.7, 0.7 ppb], b) ΔX_{GRE} [-1, 1 ppb], c) $\Delta \Delta X_{EPI}$ and d) $\Delta \Delta X_{GRE}$ slices, corresponding to visual activation area, (red rectangle in Fig.1)

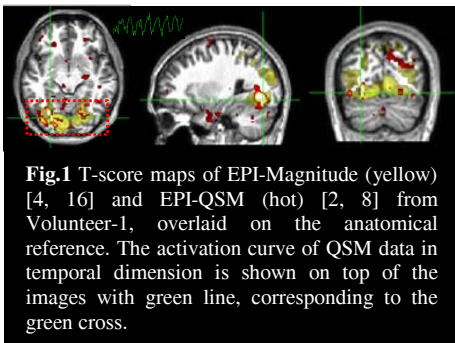


Fig.1 T-score maps of EPI-Magnitude (yellow) [4, 16] and EPI-QSM (hot) [2, 8] from Volunteer-1, overlaid on the anatomical reference. The activation curve of QSM data in temporal dimension is shown on top of the images with green line, corresponding to the green cross.

Conclusion While larger partial volume effects might partially cause the lower effect observed with the EPI data of lower spatial resolution, the difference in the sagittal sinus seems unlikely to be sufficiently explained by such an assumption⁶. Although superior image quality of the GRE data is gained at the cost of a lower temporal resolution, the preliminary results showed that GRE data may offer valuable complementary information to EPI in functional susceptibility studies targeted at the venous vessel tree. A number of previous studies have worked on suppression of venous signals^{11,12}, however; nowadays it becomes possible to continue the pioneering work done by Haacke and co-workers¹³. Functional QSM with 3D GRE sequence might have a potential use for studies including venography¹⁴ and studies with an interest in imaging veins draining neuronally activated regions. **References:** [1] Rowe and Logan. NeuroImage (2004) [2] Biancardi et al. HBM (2013) [3] Balla et al. NeuroImage (2014) [4] Özbay et al., #3170 Proc. ISMRM 2014 [5] Özbay et al., #22 3rd QSM Workshop [6] Sun and Wilman. MRM 2014 [7] Haacke et al. Neuroimage (2012) [8] Schweser et al. MRM (2013) [9] Özbay et al., #3171 Proc. ISMRM 2014 [10] SPM analysis toolbox (UCL, London, UK) [11] Duong et. al, MR (2003) [12] Glover et. al, MRM (1996) [13] Haacke et. al, NMR Biomed. (1994) [14] Fan et. al, MRM (2014)